This journal is (c) The Royal Society of Chemistry 2010

Supplementary Information

Highly Conducting Two-Dimensional Copper(I) 4-Hydroxythiophenolate Network

Kam-Hung Low,[a] V. A. L. Roy,[b] Stephen Sin-Yin Chui,[a] Sharon Lai-Fung Chan,[a] and Chi-Ming Che*[a]

[a] *Institute of Molecular Functional Materials, Department of Chemistry and HKU-CAS Joint Laboratory on New Materials, The University of Hong Kong, Pokfulam Road, Hong Kong SAR. Fax: 852 2857 1586; Tel: 852 2859 2154; E-mail: cmche@hku.hk*
[b] *Department of Physics and Materials Science, City University of Hong Kong, Tat Chee Avenue, Kowloon, Hong Kong SAR*

Instrumentation. Scanning electron microscopic (SEM) image was recorded by LEO 1530 scanning electron microscope. Transmission electron microscopic (TEM) image and selected area electron diffraction (SAED) pattern were recorded by FEI Philips Tecnai 20 transmission electron microscope. Elemental analyses of solid samples were performed at the Institute of Chemistry, Chinese Academy of Sciences.

Structural determination using powder XRD data. *a) Sample preparation and data collection:* The freshly prepared solid sample of CuHT was ground into fine powder and was loaded onto a glass holder or a sealed glass capillary. Replicate X-ray diffraction datasets were collected in a Bragg-Brentano reflection or Debye-Scherrer capillary transmission geometry by Bruker D8 ADVANCE X-ray diffractometer (λ(CuKα) = 1.5418 Å, rated as 1.6 kW). Data collection was performed with the following: 2θ range = 3–60º, step size = 0.02° in 2θ, speed of scan = 10 second/step. The phase-purity of the solid sample of CuHT was checked by ICDD (International Center for Diffraction Data, PDF-2 Release 2004) database match search and the sample in both cases were found to be free of Cu_2O.

b) Structure solution: Using Indexing program DICVOL04[s1] and/or TREOR,[s2] calculation based on the first 10 XRD maxima gave a reduced orthorhombic lattice [a = 14.466(2) Å, b = 5.127(2) Å, c = 3.991(2) Å, V = 296.03 Å^3, M(10) = 41.7, F(10) = 47.0] or monoclinic unit cell: [a = 5.123(6) Å, b = 14.469(5) Å, c = 3.989(8) Å, β = 90.240º, V = 295.78 Å^3, M(10) = 33.4, F(10) = 38.7]. The orthorhombic unit cell with double the length of a-axis was more likely to be the correct cell because a higher priority is preferred for the higher metric symmetry in the former one and the orthorhombic space group $P2_12_12_1$ is very common, leading a success in solving this structure with one formula mass unit of [CuHT] per asymmetric unit. Initial lattice

parameters were refined by Pawley fit algorithm.[s3] Background, zero-point, and profile shape parameters were refined together to achieve the improved profile fitting (reliability indicator $\chi <$ 2–5). In addition, the space group $P2_12_12_1$ (number 19) was chosen for CuHT because (i) all observable XRD peaks could be indexed and matched with the calculated Bragg peak positions, (ii) high occurrence (18216 times for $P2_12_12_1$, 970 times for $P2_12_12$) appeared in Cambridge Structural Database (CSD 2005 release). According to its unit cell volume (592.06 $Å^3$), one formula mass units of CuHT were used per asymmetric unit. Initial model for structure solution was built and written as a MOL file format by the program ISIS DRAW version 2.14, which was later converted to sets of fractional coordinates written in a Z-MARTIX file format by program Babel (http://www.eyeopen.com/babel/) or OPENBABEL (http://openbabel.sourceforge.net). Bond distances restraints (Å) were: C(sp^2/sp^3)-H 0.96, O(sp^3)-H 0.86, C(sp^2)-O(sp^3) 1.38, C(sp^2)-C(sp^2) 1.39, C(sp^2)-S 1.78, and Cu-S 2.25 Å. Bond angle restraints were 120° for C(sp^2)-C(sp^2)-C(sp^2), O(sp^3)-C(sp^2)-C(sp^2) and C(sp^2)-C(sp^2)-S, 109.5° for Cu-S-C(sp^2). The positions of carbon and hydrogen atoms of the phenyl rings were constrained into the same plane.

Structure solution calculations were initiated by a global optimization of XRD pattern using simulated annealing implemented in program DASH[s4]. A large number of trial structures (~10,000) were calculated using default parameters/setting. A total of six positional parameters (XYZ) for the CuHT fragment, and four orientation angles of the S-ligand were varied. The ∠Cu–S–C was fixed at around 109° and the torsion angle ∠Cu–S–C–C was allowed to be freely varied. When the calculated χ^2 was reduced to a minimal level (*ca.* within 5 times of the original profile χ^2 value), the structure was solved. Selected structure solutions were examined and judged based on chemical and physical knowledge as well as the graphical fit between the calculated and experimental XRD patterns.

c) Structural refinement: Prior to any structural refinement, the chemically sensible structure solution was manually adjusted so as to remove those unrealistic close non-bonded contacts by applying the appropriate sets of atom-atom distance restraints (minimum non-bonded distances of 2.0 Å and 2.5 Å for H···H and H···C respectively). For instance, when those bad contacts disappeared, the corresponding weighing factors of those distance restraints were reduced accordingly or the restraints were removed. The model adjustment process was repeated many times until there were no overlapped atoms or unrealistic bad contacts for non-bonded atoms. Subsequent Rietveld profile refinement by the full matrix least squares was carried out by

GSAS/EXPGUI suite programs.[s5] Scattering factors, corrected for real and imaginary anomalous dispersion terms were taken from the internal library of GSAS. Overall scale factor and the coefficients of the linear interpolation background function were refined. Profile shape parameters (Pseudo-Voigt function),[s6] instrumental parameters (S/L) and (H/L), sample displacement (shft), Gaussian peak width (GW) and the Lorentzian peak broadening factor due to the microstrain effect of crystallites (LY) were sequentially refined. When the refinement of all these non-structural parameters became converged with a negligible $(\text{shift/esd})^2$ value, the model-biased profile refinement was switched in which the unit cell parameters (*a, b, c* and *β*), atomic coordinates, background, peak profile parameters were refined together to give the final $R_p = 0.0698$, $R_{wp} = 0.0973$, $R_{exp} = 0.0637$ and $R_F = 0.0858$. Crystallographic data (excluding structure factors) for CuHT has been deposited in the Cambridge Crystallographic Data Center (CCDC) as supplementary publication numbers: CCDC 782395. Copies of these data can be obtained free of charge on application to CCDC, 12 Union Road, Cambridge CB2 1EZ, UK (fax: (+44) 1223-336-033; e-mail: deposit@ccdc.cam.ac.uk). Graphical plot of the final refinement cycle is shown in Figure S1.

The same procedure for sample preparation and data collection were used for CuSPh-3-OH. Indexing was based on the first 13 diffraction maxima from the diffractograph of the sample gave a reduced cubic lattice [a = 13.369(2) Å, V = 1892.46 Å^3, $M(13)$ = 41.8, $F(13)$ = 39.4], two tetragonal lattices [a = 12.362(7) Å, c = 3.573(3) Å, V = 546.13 Å^3, $M(13)$ = 52.2, $F(13)$ = 49.0 and a = 12.367(6) Å, c = 3.914(4) Å, V = 598.73 Å^3, $M(13)$ = 43.3, $F(13)$ = 41.0] and a orthorhombic lattice [a = 12.354(7) Å, b = 12.371(5) Å, c = 3.572(9) Å, V = 546.11 Å^3, $M(13)$ = 36.8, $F(13)$ = 34.8]. The tetragonal unit cell with double the length of *a*-axis was assigned by the comparison of the predicted peak positions and the observed peaks. $I4_1/a$ was chosen for the Pawley refinement and preliminary simulated annealing. Initial result showed a 1-D structure of the CuSPh-3-OH complex similar to that of CuSPh.

Four-point probe measurements

Pellets of CuHT powder with a diameter of 1 cm were prepared under a force of 8 tons. The resultant pellets were transferred into a nitrogen glove box with an environment of less than 0.1 ppm for both water and oxygen. It was loaded on a four point probe stage for measurements.

The two outer probes source current, while the two inner probes sense the resulting voltage drop across the sample. The contact resistance between the probes and the pellet which could be observed from the I-V plots is not significant. The volume resistivity is calculated with this equation:

$$\rho = \frac{\Pi}{\ln 2} \times \frac{V}{I} \times t \times k$$

where: ρ = volume resistivity (Ω-cm)

V = the measured voltage (volts)

I = the source current (amperes)

t = the sample thickness (cm)

k = a correction factor based on the ratio of the probe spacing to wafer diameter and on the ratio of wafer thickness to probe spacing[1]. These four point probe measurements were done by using different SMU (Source Measuring Units) of K4200 semiconductor parameter analyzer.

FET Device Fabrication and Charge Mobility Measurement

A common substrate-gate structure field effect transistor (FET) was fabricated. Gate oxide SiO_2 layer (100 nm, relative permittivity = 3.9) was thermally grown on heavily doped *n*-type Si substrate (gate electrode). An image reversal photolithography technique was used to form an opening on the photoresist layer for the source and drain patterns on the gate oxide. Source and drain metal layers, consisting of Ti adhesion film (10 nm, lower) and Au conductive film (50 nm, upper), were deposited by thermal evaporation. The channel length and width of the devices were 2 and 100 μm respectively. After metal film deposition, a standard lift-off process in acetone was used to remove the metal film on top of the photoresist pattern, leaving behind the Ti/Au source/drain contact patterns. A suspension of solid sample of CuHT or CuAT in methanol was ultrasonicated for more than 12 hours to disperse the solid in the solution. Later the dispersed solids were drop cast on the top of patterned bottom contact FET device. The transistor output and transfer characteristics were measured with a probe station using a Keithley K4200 semiconductor parameter analyzer inside a MBraun nitrogen glove box where oxygen and moisture level were kept below 0.1 ppm. Although a non-saturating behaviour was found for these FET devices, a clear effect of the gate on the current was observed. Since the saturation

of the drain current was not attained, the charge-carrier mobility was extracted from the linear regime using $I_{D,lin}$ vs. V_G relation [s7]. At the linear regime where $V_{DS} \ll V_{GS}$,

$$\mu = \frac{\partial I_{ds} / \partial V_{gs} L}{W C_{ox} V_d}$$

(where W is the channel width; L is the channel length; C_i is the capacitance of the SiO_2 insulating layer; V_{GS} is the gate voltage and V_t is the threshold voltage).

[s1] A. Boultif, D. Löuer, *J. Appl. Crystallogr.*, 2004, **37**, 724–731.

[s2] P. -E. Werner, L. Eriksson, M. J. Westdahl, *J. Appl. Crystallogr.*, 1985, **18**, 367–370.

[s3] G. S. Pawley, *J. Appl. Crystallogr.*, 1981, **14**, 357–361.

[s4] W. I. F. David, K. Shankland, *DASH, Program for Structure Solution from Powder Diffraction Data*, Cambridge Crystallographic Data Center, Cambridge, 2001, (License agreement No: D/1023/2002).

[s5] (a) A. C. Larson, R. B. Von Dreele, *"General Structure Analysis System (GSAS)", Los Alamos National Laboratory Report LAUR 86-748*, 2004. (b) B. H. Toby, *EXPGUI, A Graphical User Interface for GSAS*, *J. Appl. Crystallogr.*, 2001, **34**, 210–221.

[s6] (a) P. Thompson, D. E. Cox, J. B. Hastings, *J. Appl. Crystallogr.*, 1987, **20**, 79–83. (b) L. W. Finger, D. E. Cox, A. P. Jephcoat, *J. Appl. Crystallogr.*, 1994, **27**, 892–900.

[s7] S. M. Sze, *Physics of Semiconductor Devices,* second edition, Wiley, New York, 1981, 431.

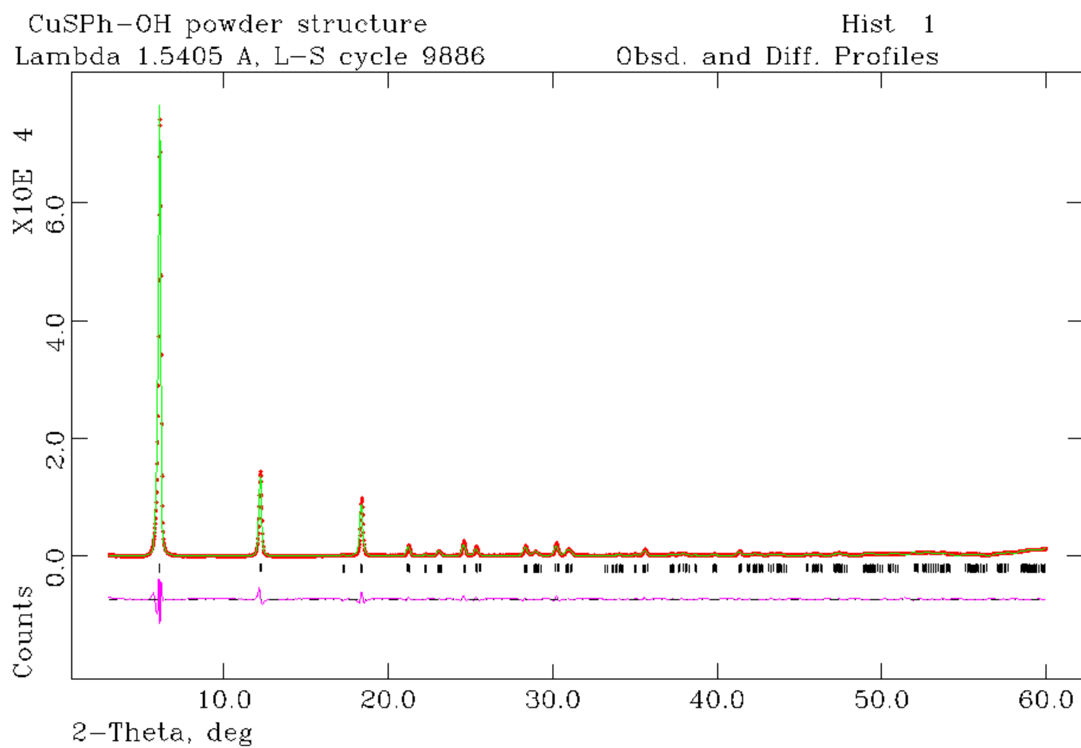

Figure S1. Graphical plot of the final Rietveld refinement cycle for CuHT (red crossed signs = observed data points, green line = calculated profile, vertical ticks = Bragg peak positions). Difference plot (magenta) between the experimental and calculated XRD patterns is shown at the bottom.

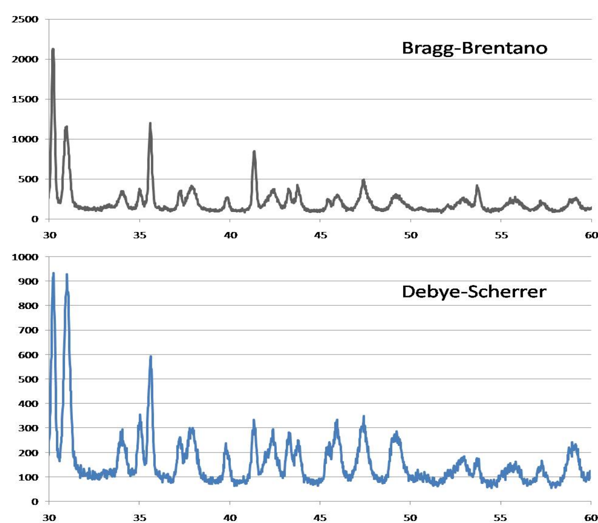

Figure S2. Enlarged diffractographs of the two collection modes at high two-theta range (30 – 60°).

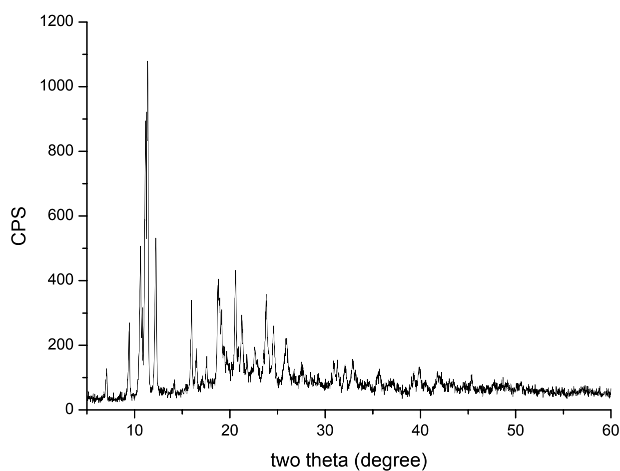

Figure S3. XRD patteren of CuAT film on glass substrate.

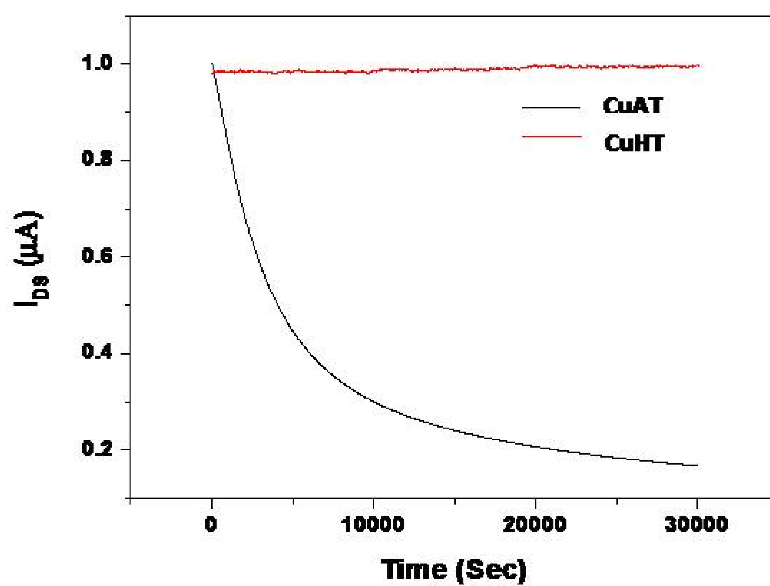

Figure S4. Transient measurements of CuHT and CuAT